A Low Cost of Burning Raw Material For PO_4^{3-}-P And F^- Solidification/Stabilization In Phosphogypsum

Li Bing
Yangtze Normal University
Shu Jiancheng (sjcees@126.com)
Southwest University of Science and Technology
Chen Mengjun
SWUST: Southwest University of Science and Technology
Zeng Xiangfei
SWUST: Southwest University of Science and Technology
Liu Renlong
Chongqing University

Research Article

Keywords: Phosphogypsum, Burning raw material, PO43--P, F-, Stabilization

Posted Date: May 10th, 2021

DOI: https://doi.org/10.21203/rs.3.rs-346383/v1

Abstract

Phosphogypsum (PG) contains a lot of soluble phosphate (PO_4^{3-}-P) and fluorine ion (F^-), which seriously has hindered the sustainable development of phosphorous chemical industry. In this study, a new burning raw material (BRM) was used for the stabilize of PO_4^{3-}-P and F^- in PG. The characteristics of PG and BRM, stabilize mechanism of PO_4^{3-}-P and F^-, leaching test and economic evaluation were investigated. The effect of PG and BRM weight ratio, solid to liquid ratio, reaction time and reaction temperature on the concentrations of PO_4^{3-}-P and F^- were studied. The results showed that the concentration of F^- in PG leaching solution was 8.65 mg/L and the removal efficiency of PO_4^{3-}-P was 99.78 %, as well as the pH of PG leaching solution was 8.12, when the weight ratio of PG and BRM was 100:2, and the solid to liquid ratio was 4:1, reacting for 24 h at the temperature of 30 °C. PO_4^{3-}-P and F^- were mostly solidified as $Ca_5(PO_4)_3F$, $CaPO_3(OH)$, $Ca_5(PO_4)_3(OH)$, $Ca_2P_2O_7{\cdot}2H_2O$, $CaSO_4PO_3(OH){\cdot}4H_2O$, CaF_2, and $CaFPO_3{\cdot}2H_2O$. Leaching test results indicated that the concentrations of PO_4^{3-}-P, F^- and heavy metals were less than the integrated wastewater discharge standard (GB8978-1996). Economic evaluation revealed that the cost of PG treatment was $ 0.88/ton. This study provides a new low cost and harmless treatment method for PG.

Introduction

Phosphogypsum (PG) is a industrial solid waste produced in the production of phosphate fertilizer and phosphoric acid (Zhong et al.,2020; Zhou et al.,2020; Zmemla et al.,2020). Nowadays, the world's annual PG emissions amount to 280 million tons, China has also exceeded 50 million tons (Yang et al.,2020). POFTs are mainly composed of $CaSO_4{\cdot}2H_2O$, quartz, undecomposed apatite, soluble PO_4^{3-}-P (PO_4^{3-}, HPO_4^{2-}, $H_2PO_4^-$, H_3PO_4), F^-, SO_4^{2-}, Mg^{2+}, silica-calcium salt, organic matters and silica-aluminum salt(Wang et al.,2020; Masmoudi et al.,2020; Zhang et al.,2020; Narloch et al.,2019), and it also contains small amounts of heavy metals (Al-Hwaiti et al.,2019; Saueia et al.,2020). Some PG contains radium 226, thorium 232 and potassium 40 radionuclides (Ajam et al.,2020; Kuzmanovic et al.,2020; Gijbels et al.,2019). At present most PG is still used for landfill disposal.

Many studies has focused on resource utilization of PG, such as saline-alkali soil improver (Pukalchik et al.,2019), mineral addition in cement industry (Rosales et al.,2020; Ennaciri et al.,2020), non-autoclaved aerated concrete (Wang et al.,2020), cementitious materials (Sun et al.,2020), backfill material for underground mine (Xue et al.,2020) self-leveling mortar (Yang et al.,2016; Criado et al.,2019), brick production (Turkel et al.,2012), gypsum ceiling (Kanno et al.,2008), carbonation product (Ding et al.,2019; Ding et al.,2019), and gypsum mortar ingredients (Mihelj et al.,2013). Syngas from PG and low-quality lignite is also a research hotspot (Yang et al.,2019). But these methods have not completely achieved the resource utilization of PG, because the water-soluble PO_4^{3-}-P (PO_4^{3-}, HPO_4^{2-}, $H_2PO_4^-$, H_3PO_4) and F^- content in PG corrodes the equipment and reduces the gypsum strength. A large number of scholars has studied the pretreatment of PG, such as washing (Lokshin et al.,2015), wet sieve vortex flow process (Ennaciri et al.,2020), quicklime neutralization treatment (Gu et al.,2020; Li et al.,2019), among them, .quicklime is commonly used for the harmless treatment of PG, in which PO_4^{3-}, HPO_4^{2-}, $H_2PO_4^-$, and F^- reacted with Ca^{2+} to forms of $Ca_3(PO_4)_2$, $CaPO_3(OH){\cdot}2H_2O$, $Ca(H_2PO_4)_2$, and CaF_2. Quicklime method is simple process, no external drainage, economic and environmental protection in the production of gypsum board or cement retarder were application. But the price of quicklime was higher than a new alkaline reagents of burning raw material (BRM), and the concentration of PO_4^{3-}-P still is higher than the integrated wastewater discharge standard (GB8978-1996) (Shu et al.,2020).

PG will produce a lot of PO_4^{3-}-P and F^- leachate during the storage process. Water contaminated with PO_4^{3-}-P and F^- is harmful to human health and environment. Too much PO_4^{3-}-P can lead to contact dermatitis, harm to marine life, soil pollution and deterioration of water quality (Shaddel et al.,2020). F^- will disrupts the normal metabolism of calcium and phosphorus, and damages teeth, heart muscle and skeletal muscle (Shu et al.,2020). Therefore, it is urgent to find a low cost alkaline material for PO_4^{3-}-P and F^- solidification/stabilization in PG.

BRM is a intermediate product in the cement production process (Huang et al.,2020). The content of CaO in BRM was higher than 75%, and nanoscale CaO materials has high reactivity, and burning SiO_2, Al_2O_3 and Fe_2O_3 in the BRM can further improve the activity of the BRM. In this study, BRM was used for the PO_4^{3-}-P and F^- stabilize in PG. The effects of different solid to liquid ratio, reaction time, and reaction temperature on the concentrations of PO_4^{3-}-P and F^- were investigated. The stabilization/solidification mechanism of PO_4^{3-}-P and F^- was studied. Leaching test and economic evaluation were investigated. This study provided a new research idea for PG harmless disposal.

Materials And Method

2.1 Materials

The PG sample was collected from Chongqing province in China, and the water content of PG was 12 %. BRM was supplied from Guizhou province in China. Different perpendicular depth of 300 mm in the PG landfill was chosen as sampling points. BRM and stabilized samples for dried to a constant weight at 60 °C. NaOH, H_2SO_4, $KNaC_4H_4O_6{\cdot}4H_2O$, $K_4O_7P_2$, $C_2H_3NaO_2{\cdot}3H_2O$ were purchased from Mianyang xinjie trading co. LTD, China (Analytical grade). Water Purification System (HMCWS10) provided the deionized water in this study. The PG radioactivity in this experiment were tested (Each sample was tested in three parallel groups). As shown in Table 1 of the supporting information, both the internal and external exposure indexes (IRa, Ir) of PG were less than the standard of building materials radionuclide limit (GB 6566 – 2010. IRa ≤ 1.0, Ir ≤ 1.3). Therefore, the activity concentration of the radionuclides in PG was not measured in leaching process.

Table 1 Mean values of phosphogypsum internal and external exposure indices

	Phosphogypsum	
	IRa	Ir
No:001	0.525(±12.92%)	0.495(± 8.10%)
No:002	< 0.272	< 0.180
No:003	< 0.266	< 0.172
Average value	< 0.354	< 0.282
Standard:GB6566-2001 (Grade A Finishing material)	IRa≤1.0	Ir≤1.3

2.2 Experimental process

Firstly, PG and BRM were mixed well for 30 min, and the effects of PG and BRM weight ratio (100:0.7 to 100:3) on the concentrations of PO_4^{3-}-P and F^- in PG sample were investigated when the solid to liquid ratio was 4:1 and the temperature at 30 ℃. Secondly, an appropriate amount of distilled water (weight of water to EMB) was added at the different solid to liquid ratio of BRM and PG (PGB) and water (3:1 to 6:1), when the weight ratio of PG and BRM was 4:1 and the temperature at 30 ℃. The mixture of PGB and water were mixed at high speed for 30 min, and then the S/S samples was carried out at different temperature (20 ℃ to 40 ℃), when the weight ratio of PG and BRM was 4:1, and the solid to liquid ratio of PGB and water was 4:1. Finally, the pH of S/S samples leaching solution, and the concentrations of PO_4^{3-}-P and F^- were determined at set time.

2.3 Analysis methods

Leaching test was determined by Solid waste-Horizontal vibration method (China HJ557—2010). The concentration of heavy metals in BRM and PG leaching solution were test by inductively coupled plasma optical emission spectrometer (ICP-OES; Thermo Fisher scientific, ICAP 6500, USA). PO43– P was determined by ammonium molybdate spectrophotometry, and F- was determined by fluoride ion selective electrode method. Ultra-trace sample volume-type pH electrode (PHSe3C, Shanghai, China) was used to test the pH of leaching solution. FT-IR spectra was obtained by Magna 550II FT-IR spectrometer (PerkinElmer Frontier) via the KBr pellet method. Phase composition, microstructure and composition of PG, BRM and stabilized samples were analyzed by X-ray diffractometer (XRD; JapanD/max-IIIA), Scanning Electron Microscopy (SIgma 300), X-ray spectroscopy system (EDS; ΣIGMA + X-Max20, Zeiss, Germany), and X-ray fluorescence (XRF; PANalytical B.V., Axios; Netherlands), respectively.

Results And Discussion

3.1 Characteristics of PG and BRM

PG mainly consists of CaO, SO_3 and SiO_2, all of which accounts for about 94.57 % of the total composition (Table 2). In Fig. 1a, the X-ray powder diffraction shows that PG mainly contains $CaSO_4{\cdot}2H_2O$ and SiO_2, $CaPO_3(OH){\cdot}2H_2O$, $Ca_3(PO_4)_2$, $CaPO_3(OH)$, and $Ca_2P_2O_7{\cdot}4H_2O$. BRM mainly contains of CaO, SiO_2, MgO, Al_2O_3, Fe_2O_3, and SO_3, which accounts for about 95.59 % of the total composition. This results can be further confirmed by other study (Jin et al.,2020). X-ray powder diffraction of BRM was further confirmed that BRM mainly contains SiO_2, CaO, $Ca(OH)_2$, $CaH_2(SO_4)$, $CaAl_2Si_2O_8{\cdot}4H_2O$, $Ca_3(SiO_3OH)_2{\cdot}4H_2O$, FeOOH, $Al_2O_3{\cdot}4H_2O$, and $Al(OH)_3$ in Fig. 1b. The above results confirmed that most Mg^{2+}, Ca^{2+}, F^-, and PO_4^{3-}-P in PG exist in stable crystalline form, and BRM can be dissolved in water as alkaline agents to adjust the pH. In Fig. 1c, SEM images of BRM also showed that relatively uniform particles with a particle size range from 300 nm to 500 nm. A high magnification SEM image of PG reveals that flake morphology with a particle size range from 50 μm to 80 μm, and the surface content of precipitate particles mainly contains of O, Ca, S, C, F, Mg, P, and Al according to EDX analysis (In Fig. 1d).

Table 2 Chemical compositions of the PG and BRM (wt. %)

	MgO	SiO_2	CaO	Al_2O_3	Fe_2O_3	SO_3	TiO_2	P_2O_5	MnO	SrO	K_2O	F	Other
PG	0.35	2.35	44.37	0.48	0.131	47.85	0.046	1.67	*	0.071	0.07	2.42	0.192
BRM	1.51	8.42	75.42	2.86	3.61	3.77	0.47	0.23	0.04	0.17	0.99	*	1.86

* Not detected.

As shown in Table 3 of the supporting information, the pH of the PG leaching solution and BRM leaching solution were 2.67 and 12.3, respectively, which did not met the integrated wastewater discharge standard (GB8978-1996). The concentrations of Se^{4+}, PO_4^{3-}, and F^- in PGL were 1.557 mg/L, 209.52 mg/L and 46.21 mg/L, respectively, all of which were higher than the integrated wastewater discharge standard (GB8978- 1996), and trace amounts of Pb^{2+}, Zn^{2+}, Ni^{2+}, Cu^{2+}, Cr^{6+}, Cd^{2+}, Co^{2+}, Mn^{2+}, and Ba^{2+} also existed in PG. The concentrations of Mg^{2+} and Ca^{2+} were 53.77 mg/L and 602.0 mg/L in PG, respectively. The concentrations of Zn^{2+} in BRM leaching solution was higher than the integrated wastewater discharge standard (GB8978-1996), and the concentrations of Mg^{2+} and Ca^{2+} were 6.45 mg/L and 879.1 mg/L in BRM, respectively. The results showed that BRM can be provide high concentrations of OH^- and Ca^{2+}, when BRM used as an alkaline agent to stabilize PO_4^{3-} and F^- in PG.

Table 3 Different ion concentration of the PG and BRM (mg/L)

	pH	Pb^{2+}	Zn^{2+}	Cu^{2+}	Ni^{2+}	Fe^{2+}	Mg^{2+}	Se^{4+}	Ca^{2+}	Cr^{6+}	Cd^{2+}	Co^{2+}	Ba^{2+}	Mn^{2+}	PO_4^{3-}-P	F^-
PG	2.67	0.316	0.438	0.661	0.302	3.3	53.77	1.557	602	0.081	0.014	0.22	0.132	1.33	209.52	4621
BRM	12.3	0.237	4.425	0.036	0.082	*	6.45	0.698	879.1	*	0.08	0.021	0.878	0.845	*	*
GB8978-1996	6~9	1.0	2.0	0.5	1.0	/	/	0.2	/	0.5	0.1	/	1.0	2	0.5	10

* Not detected.

3.2 Effect of PG and BRM weight ratio

In Fig. 2a, the pH of leaching solution increased with the weight ratios of PG and BRM increased at the given reaction time, due to the concentration of OH^- increased with the dosage of BRM increased; And the pH not much has changed with the reaction time was higher than 5 h, at the given PG and BRM weight ratio. The pH was less than 9.00, which meet the integrated wastewater discharge standard (GB8978-1996), when the weight ratios of PG and BRM was 100:2 and reaction time was higher than 5 h. Figure 2b showed that the removal efficiency of PO_4^{3-}-P increased as the weight ratios of PG and BRM increased from 100:0.7 to 100:3 at a given reaction time. The concentration of PO_4^{3-}-P was higher than the integrated wastewater discharge standard (GB8978-1996) when the reaction time was less than 24 h at any PG and BRM weight ratios. In Fig. 2c, the concentration of F^- decreased with the weight ratios of PG and BRM increased at a given reaction time, due to F^- was began to react with Ca^{2+} and Mg^{2+} to form fluoride precipitation with the pH of leaching solution increase (Sengupta et al.,2020; Borgohain et al.,2020); At a given PG and BRM weight ratios, the concentration of F^- decreased with the reaction time increased. Considering the concentration of F^-, and the removal efficiency of PO_4^{3-}-P, as well as economic costs in the S/S system. The weight ratios of PG and BRM was 100:2 and reacting for 24 h were selected as the optimal reaction condition.

3.3 Effect of solid to liquid ratio and reaction temperature

In Fig. 3a, the concentration of F^- decreased with the solid to liquid ratio decreased at a given reaction time, because more Ca^{2+} in BRM began to react with F^- to form fluoride precipitation with the solid to liquid ratio decreased (Wei et al.,2020). The concentration of F^- decreased as the increased reaction time at a given PG and BRM weight ratio. At a given solid to liquid ratio, the removal efficiency of PO_4^{3-}-P increased with as the increased of reaction time (Fig. 3b), due to PO_4^{3-}-P in the solution forms phosphate precipitate with Ca^{2+} and Mg^{2+} in BRM (Muisa et al.,2020; Wang et al.,2020); the removal efficiency of PO_4^{3-}-P increased with the solid to liquid ratio decreased from 6:1 to 3:1 at a given reaction time. The concentration of F^- was 8.65 mg/L, and the removal efficiency of PO_4^{3-}-P was 99.78 %, respectively, when the solid to liquid ratio was 4:1 and reaction for 24 h at 30℃. The above results showed that low solid to liquid ratio was favorable for F^- and PO_4^{3-}-P removal. Considering the moisture content of PG in phosphorous chemical industry. The solid to liquid ratio at 4:1 was selected as the optimal condition.

In Fig. 3c, the concentration of F^- decreased with the increased of reaction temperature at a given reaction time, because F^- began to react with Ca^{2+} and Mg^{2+} to form fluoride precipitation with the temperature increased; At a given reaction temperature, the concentration of F^- decreased as the increased of reaction times. As shown in Fig. 3d, the removal efficiency of PO_4^{3-}-P increased when the reaction temperature increased from 20 ℃ to 40 ℃, because PO_4^{3-}-P began to react with Ca^{2+} and Mg^{2+} to form phosphate precipitation (Qiu et al.,2020). According to the concentration of F^-, and the removal efficiency of PO_4^{3-}-P, as well as economic costs in the S/S system. The solid to liquid ratio was 4:1 and reaction temperature at 30 ℃ were selected as the optimal reaction condition.

3.4 Stabilize mechanism of PO_4^{3-}-P and F^-

The main mineralogical components of precipitate mainly were gypsum ($CaSO_4{\cdot}2H_2O$), brushite ($CaPO_3(OH){\cdot}2H_2O$), SiO_2, Ca_3PO_4, $CaPO_3(OH)$, $Ca_2P_2O_7{\cdot}4H_2O$, $Ca_5(PO_4)_3F$, $CaPO_3(OH)$, $Ca_5(PO_4)_3(OH)$, $Ca_2P_2O_7{\cdot}2H_2O$, $CaSO_4PO_3(OH){\cdot}4H_2O$, CaF_2 and $CaFPO_3{\cdot}2H_2O$ (Vasconez-Maza et al.,2019), when the weight ratios of PG and BRM increased from 100:0.7 to 100:3 reacting for 24 h at 30 ℃ (Fig. 4). The intensity of diffraction peak of $CaSO_4{\cdot}2H_2O$, $Ca_5(PO_4)_3(OH)$ and SiO_2 decreased when the weight ratios of PG and BRM changed from 100:0.7 to 100:3, because soluble PO_4^{3-}-P and F^- react with Ca^{2+} and Mg^{2+} in BRM to forms of phosphate precipitation (Romero-Hermida et al.,2019) and fluoride precipitation, and these deposited small particles cover the surface of $CaSO_4{\cdot}2H_2O$, $Ca_5(PO_4)_3(OH)$, and SiO_2. A small number of new characteristic peaks of $Ca_5(PO_4)_3F$, $CaPO_3(OH)$, $Ca_5(PO_4)_3(OH)$, $Ca_2P_2O_7{\cdot}2H_2O$, $CaSO_4PO_3(OH){\cdot}4H_2O$, CaF_2, and $CaFPO_3{\cdot}2H_2O$ appear compare with raw PG. The above result showed that PO_4^{3-}-P and F^- in PG were mainly removed by $Ca_5(PO_4)_3F$, $CaPO_3(OH)$, $Ca_5(PO_4)_3(OH)$, $Ca_2P_2O_7{\cdot}2H_2O$, $CaSO_4PO_3(OH){\cdot}4H_2O$, CaF_2, and $CaFPO_3{\cdot}2H_2O$, when the weight ratio of PG and BRM was 100:2 reacting for 24 h and the temperature at 30 ℃.

The surface of the large sheet structure is covered with a small amount of non-uniform impurity particles were found when the weight ratio of PG and BRM was 100:0.7 (Fig. 5a). The surface content of precipitate particles mainly contains O, Ca, S, C, F, Si, P, Al and Fe according to EDX analysis. Combined with XRD analysis results, it can be further proved that the sheet structure mainly was $CaSO_4{\cdot}2H_2O$ (Lu et al.,2019; Li et al.,2019), and non-uniform impurity particles mainly was newly formed phosphate and fluoride precipitate. The surface of the sheet structure is covered with more and more non-uniform particles with the weight ratio of PG and BRM increased from 100:1 to 100:1.5 (Fig. 5b-Fig. 5c). The results showed that more Ca^{2+} and Mg^{2+} form a precipitate with PO_4^{3-}-P and F^-. Spicules of small particles with 0.4 μm diameters appeared on the surface of the sheet particles in Fig. 5. Spicules particles appeared in Fig. 5e when the weight ratio of PG and BRM was 100:3. The surface of spicules particles structure mainly contains Ca, O, S, C, F, Si, P, Al and Fe

according to EDX analysis. Spicules particles mainly were newly formed $CaSO_4{\cdot}2H_2O$ $Ca_5(PO_4)_3F$, $CaPO_3(OH)$, $Ca_5(PO_4)_3(OH)$, $Ca_2P_2O_7{\cdot}2H_2O$, $CaSO_4PO_3(OH){\cdot}4H_2O$, CaF_2, and $CaFPO_3{\cdot}2H_2O$ according to XRD analysis.

In Fig. 6, the main peak position of the infrared spectra of the S/S samples were very similar when the weight ratios of PG and BRM increased from 100:0.7 to 100:3. Peaks at 3551 cm^{-1}, 3415 cm^{-1} and 1618 cm^{-1} could be ascribed to the bending vibration of -O-H and O-H, respectively (Shu et al.,2019). The result indicated that the S/S sample and raw PG mainly contains a large number of crystal water. The peak at 603 cm^{-1} and 476 cm^{-1} was caused by the stretching vibration of the SO_4^{2-}. XRD further confirmed that crystalline water in S/S samples mainly was $CaSO_4{\cdot}2H_2O$ (Shu et al.,2016). While those at 1116 cm^{-1} and 670 cm^{-1} could be assigned to the stretching vibration of PO_4^{3-}, and the peaks at 2244 cm^{-1} could be ascribed to the bending vibration of $H_2PO_4^-$ (Haque et al.,2020). The result showed that the sample contain a large number of phosphate precipitation. This above results can be further confirmed by XRD.

According to XRD, SEM-EDS and FT-IR analysis, and combining with the concentrations of Mg^{2+}, Ca^{2+}, PO_4^{3-}-P and F. The main reaction equations are as follows:

$CaO + H_2O \rightarrow Ca(OH)^+(surface) + OH^-$ (2)

$SiO_2 + 2OH^- \rightarrow SiO_3^{2-} + 2H_2O$ (3)

$SiO_3^{2-} + Ca^{2+-} \rightarrow CaSiO_3\downarrow$ (4)

$Ca^{2+} + SO_4^{2-} + 2H_2O \rightarrow CaSO_4{\bullet}2H_2O\downarrow$ (5)

$Ca^{2+} + 2F^- \rightarrow CaF_2\downarrow$ (6)

$3Ca^{2+} + 3PO_4^{3-} + 4H_2O \rightarrow Ca_2P_2O_7{\bullet}2H_2O\downarrow + CaPO_3(OH)\downarrow + 3OH^-$ (7)

$3F^- + Ca_5(PO_4)_3OH \rightarrow 3OH^- + Ca_5(PO_4)_3F\downarrow$ (8)

$5Ca^{2+} + F^- + 3PO_4^{3-} \rightarrow Ca_5(PO_4)_3F\downarrow$ (9)

$Ca^{2+} + PO_4^{3-} + H_2O \rightarrow CaPO_3(OH)\downarrow + OH^-$ (10)

$2Ca^{2+} + SO_4^{2-} + PO_4^{3-} + 5H_2O \rightarrow CaSO_4Ca(PO_3OH){\cdot}4H_2O\downarrow + OH^-$ (11)

3.5 Leaching test and economic analysis

Table 4 Leaching test results at different of PG and BRM weight ratio and reaction time (mg/L).

	Pb^{2+}	Zn^{2+}	Cu^{2+}	Ni^{2+}	Fe^{2+}	Mg^{2+}	Se^{4+}	Ca^{2+}	Cr^{6+}	Cd^{2+}	Co^{2+}	Ba^{2+}	Mn^{2+}	PO_4^{3-}-P	F^-	pH
PG:BRM (100:0.7) 24h	0.256	2.125	0.154	0.284	0.045	52.32	0.564	763.25	*	0.015	0.134	0.456	0.034	19.65	13.54	5.56
PG:BRM (100:1) 24h	0.235	1.345	0.136	0.282	0.025	43.24	0.498	654.52	*	0.011	0.021	0.356	0.024	17.65	10.21	7.66
PG:BRM (100:2) 12h	0.233	1.864	0.168	0.252	*	32.21	0.324	689.12	*	*	*	0.354	*	1.12	9.54	8.12
PG:BRM (100:2) 24h	0.153	1.534	0.116	0.252	*	23.54	0.331	666.32	*	*	*	0.321	*	0.45	8.65	8.12
PG:BRM (100:2) 48h	0.231	1.084	0.117	0.232	*	22.65	0.312	645.21	*	*	*	0.278	*	0.42	6.35	8.05
PG:BRM (100:3) 24h	0.124	0.958	0.086	0.181	*	26.32	0.235	777.35	*	*	*	*	*	0.34	6.57	9.25
GB8978-1996	1.0	2.0	0.5	1.0	/	/	0.2	/	0.5	0.1	/	1.0	2	0.5	10	

* Not detected.

The concentrations of Pb^{2+}, Zn^{2+}, Cu^{2+}, Ni^{2+}, Fe^{2+}, Se^{4+}, Cr^{6+}, Cd^{2+}, Co^{2+}, Ba^{2+}, and Mn^{2+} were less than the integrated wastewater discharge standard (GB8978-1996) in Table 4. The concentrations of Mg^{2+}, PO_4^{3-}-P and F^- decreased when the weight ratios of PG and BRM changed from 100:0.7 to 100:3 reacting for 24 h and the temperature at 30 ℃. The concentrations of Mg^{2+}, Ca^{2+}, PO_4^{3-}-P, F^-, and other heavy metals decreased with the reaction time increased from 12 h to 48 h. The concentration of Mg^{2+} decreased from 52.32 mg/L to 22.65 mg/L, and Ca^{2+} decreased from 662.39 mg/L to 645.21 mg/L when the weight ratios of PG and BRM changed from 100:0.7 to 100:3 reacting for 48 h and the temperature at 30 ℃. The results showed that Mg^{2+} can be removed by BRM. The concentrations of Mg^{2+}, Ca^{2+}, PO_4^{3-}-P, and F^- were 23.54 mg/L 666.32 mg/L, 0.45 mg/L and 8.65 mg/L, respectively, and the pH of PGB leaching solution was 8.12, which met the integrated wastewater discharge standard (GB8978-1996).
In this study, PO_4^{3-}-P and F^- S/S process was analyzed by economic viewpoint. The costs of the chemicals reagents were only considered. The price of BRM was $ 44.0/ton according to cement industry in China, and the dosage of BRM was 20 kg when treatment per ton PG. Therefore, the total cost of harmless treatment PG by BRM was $ 0.88/ton. In addition, the price of quicklime was $ 92.86 /ton in China, and the dosage of quicklime was 20 kg when treatment per ton PG, and the total cost of harmless treatment PG by quicklime was $ 1.86/ton. Moreover, the concentration of PO_4^{3-}-P in PG can only be reduced to 10 mg/L when quicklime as the stabilizing agent. The concentration of PO_4^{3-}-P in PG can be less than 0.5 mg/L when BRM as the stabilizing agent. The results indicated that the removal efficiency of PO_4^{3-}-P and the cost of PG treatment was better than that of quicklime.

Conclusion

In this study, BRM was used for PO_4^{3-}-P and F^- stabilize in PG. The result indicated that the pH of S/S samples leaching solution was 8.12, and the concentration of F^- was 8.65 mg/L, as well as the removal efficiency of PO_4^{3-}-P was 99.78 %, when the weight ratio of PG and BRM was 100:2, and the solid to liquid ratio was 4:1, reacting for 24 h at the temperature of 30 ℃. PO_4^{3-}-P and F^- were mostly solidified as $Ca_5(PO_4)_3F$, $CaPO_3(OH)$, $Ca_5(PO_4)_3(OH)$, $Ca_2P_2O_7{\cdot}2H_2O$, $CaSO_4PO_3(OH){\cdot}4H_2O$, CaF_2, and $CaFPO_3{\cdot}2H_2O$. Leaching test results indicated that the concentrations of PO_4^{3-}-P, F^-, heavy metals and the pH of S/S samples leaching solution met the integrated wastewater discharge standard (GB8978-1996). Economic evaluation revealed that the cost of PG treatment was $ 0.88/ton. This study provides a new low cost and harmless treatment method for PG.

Declarations

Acknowledgement

This work was supported by 'National Natural Science Foundation of China' (21806132), 'Chongqing science and technology innovation leading talent support program (CSTCCXLJRC201703)'.

Authors Contributions

Li Bing *Data curation, Methodology, Software.*

Shu Jiancheng : *Data curation, Writing- Reviewing and Editing, Methodology, Software.*

Chen Mengjun *Supervision.*

Zeng Xiangfei *Supervision.*

Liu Renlong *Supervision.*

Ethics approval and consent to participate

Approval was obtained from the ethics committee of Southwest University of Science and Technology. The procedures used in this study adhere to the tenets of the Declaration of Helsinki.

Consent to Publish

Informed consent was obtained from all individual participants included in the study.

Funding

All sources of funding for the research reported should be declared. The role of the funding body in the design of the study and collection, analysis, and interpretation of data and in writing the manuscript should be declared.

Availability of data and materials

All data generated or analysed during this study are included in this published article (and its supplementary information files).

Declaration of interests

 The authors declare that they have no known competing financial interests or personal relationships that could have appeared to influence the work reported in this paper.

The authors declare the following financial interests/personal relationships which may be considered as potential competing interests:

We declare that we do not have any commercial or associative interest that represents a conflict of interest in connection with the work submitted.

References

1. A. Masmoudi-Soussi, I. Hammas-Nasri, K. Horchani-Naifer, M. Ferid, Rare earths recovery by fractional precipitation from a sulfuric leach liquor obtained after phosphogypsum processing, Hydrometallurgy, 191 (2020).
2. B. Wang, G.Q. Lian, X.Q. Lee, B. Gao, L. Li, T.Z. Liu, X.Y. Zhang, Y.L. Zheng, Phosphogypsum as a novel modifier for distillers grains biochar removal of phosphate from water, Chemosphere, 238 (2020).
3. B. Li, J.C. Shu, L. Yang, C.Y. Tao, M.J. Chen, Z.H. Liu, R.L. Liu, An innovative method for simultaneous stabilization/solidification of PO_4^{3-} and F^- from phosphogypsum using phosphorus ore flotation tailings, J Clean Prod, 235 (2019) 308-316.
4. C.H.R. Saueia, M.B. Nisti, P.S.C. da Silva, J.P. de Oliveira, B.P. Mazzilli, Lixiviation of rare earth elements in tropical soils amended with phosphogypsum, Int J Environ an Ch, 100 (2020) 675-685.
5. C.Q. Wang, X.D. Mei, C. Zhang, D.S. Liu, F.L. Xu, Mechanism study on co-processing of water-based drilling cuttings and phosphogypsum in non-autoclaved aerated concrete, Environ Sci Pollut R, 27 (2020) 23364-23368.
6. D.C. Narloch, S.A. Paschuk, J.N. Correa, Z. Rocha, W. Mazer, C.A.M.P. Torres, F. Del Claro, V. Denyak, H.R. Schelin, Characterization of radionuclides present in portland cement, gypsum and phosphogypsum mortars, Radiat Phys Chem, 155 (2019) 315-318.
7. E.P. Lokshin, O.A. Tareeva, Production of high-quality gypsum raw materials from phosphogypsum, Russ J Appl Chem, 88 (2015) 567-573.
8. J. Yang, Y. Wei, J. Yang, H.P. Xiang, L.P. Ma, W. Zhang, L.C. Wang, Y.H. Peng, H.P. Liu, Syngas production by chemical looping gasification using Fe supported on phosphogypsum compound oxygen carrier, Energy, 168 (2019) 126-135.
9. J.C. Shu, M.J. Chen, H.P. Wu, B.B. Li, B. Wang, B. Li, R.L. Liu, Z.H. Liu, An innovative method for synergistic stabilization/solidification of Mn^{2+}, NH_4^+-N, PO_4^{3-} and F^- in electrolytic manganese residue and phosphogypsum, J Hazard Mater, 376 (2019) 212-222.
10. J.C. Shu, H.P. Wu, M.J. Chen, H. Peng, B. Li, R.L. Liu, Z.H. Liu, B. Wang, T. Huang, Z.B. Hu, Fractional removal of manganese and ammonia nitrogen from electrolytic metal manganese residue leachate using carbonate and struvite precipitation, Water Res, 153 (2019) 229-238.
11. J.C. Shu, R.L. Liu, Z.H. Liu, H.L. Chen, J. Du, C.Y. Tao, Solidification/stabilization of electrolytic manganese residue using phosphate resource and low-grade MgO/CaO, J Hazard Mater, 317 (2016) 267-274.
12. J. Rosales, S.M. Perez, M. Cabrera, M.J. Gazquez, J.P. Bolivar, J. de Brito, F. Agrela, Treated phosphogypsum as an alternative set regulator and mineral addition in cement production, J Clean Prod, 244 (2020).
13. J. Zhou, X.Q. Li, Y. Zhao, Z. Shu, Y.X. Wang, Y. Zhang, X. Shen, Preparation of paper-free and fiber-free plasterboard with high strength using phosphogypsum, Constr Build Mater, 243 (2020).
14. J.C. Shu, B. Li, M.J. Chen, D.Y. Sun, L. Wei, Y. Wang, J.Y. Wang, An innovative method for manganese (Mn^{2+}) and ammonia nitrogen (NH_4^+-N) stabilization/solidification in electrolytic manganese residue by basic burning raw material, Chemosphere, 253 (2020).
15. J. Yang, L.P. Ma, H.P. Liu, Z.Y. Guo, Q.X. Dai, W. Zhang, K. Bounkhong, Chemical behavior of fluorine and phosphorus in chemical looping gasification using phosphogypsum as an oxygen carrier, Chemosphere, 248 (2020).
16. K. Gijbels, S. Landsberger, P. Samyn, R.I. Iacobescu, Y. Pontikes, S. Schreurs, W. Schroeyers, Radiological and non-radiological leaching assessment of alkali-activated materials containing ground granulated blast furnace slag and phosphogypsum, Sci Total Environ, 660 (2019) 1098-1107.
17. K. Gu, B. Chen, Loess stabilization using cement, waste phosphogypsum, fly ash and quicklime for self-compacting rammed earth construction, Constr Build Mater, 231 (2020).
18. L. Ajam, A.B. Hassen, N. Reguigui, Phosphogypsum utilization in fired bricks: Radioactivity assessment and durability, J Build Eng, 26 (2019).
19. L. Yang, Y.S. Zhang, Y. Yan, Utilization of original phosphogypsum as raw material for the preparation of self-leveling mortar, J Clean Prod, 127 (2016) 204-213.
20. L.F. Wei, F. Zietzschmann, L.C. Rietveld, D. van Halem, Fluoride removal by Ca-Al-CO_3 layered double hydroxides at environmentally-relevant concentrations, Chemosphere, 243 (2020).
21. L. Qiu, P. Zheng, M. Zhang, X.Q. Yu, A. Ghulam, Phosphorus. removal using ferric-calcium complex as precipitant: Parameters optimization and phosphorus-recycling potential, Chem Eng J, 268 (2015) 230-235.
22. M. Al-Hwaiti, K.A. Ibrahim, M. Harrara, Removal of heavy metals from waste phosphogypsum materials using polyethylene glycol and polyvinyl alcohol polymers, Arab J Chem, 12 (2019) 3141-3150.
23. M. Criado, D.M. Bastidas, V.M. La Iglesia, A. La Iglesia, J.M. Bastidas, Precipitation mechanism of soluble phosphates in mortar, Eur J Environ Civ En, 23 (2019) 1265-1274.
24. M.I. Romero-Hermida, A.M. Borrero-Lopez, F.J. Alejandre, V. Flores-Ales, A. Santos, J.M. Franco, L. Esquivias, Phosphogypsum waste lime as a promising substitute of commercial limes: A rheological approach, Cement Concrete Comp, 95 (2019) 205-216.
25. M.D. Vasconez-Maza, M.A. Martinez-Segura, M.C. Bueso, A. Faz, M.C. Garcia-Nieto, M. Gabarron, J.A. Acosta, Predicting spatial distribution of heavy metals in an abandoned phosphogypsum pond combining geochemistry, electrical resistivity tomography and statistical methods, J Hazard Mater, 374 (2019) 392-400.

26. M.A. Pukalchik, A.M. Katrutsa, D. Shadrin, V.A. Terekhova, I.V. Oseledets, Machine learning methods for estimation the indicators of phosphogypsum influence in soil, J Soil Sediment, 19 (2019) 2265-2276.
27. M.A. Haque, B. Chen, Y.T. Liu, S.F.A. Shah, M.R. Ahmad, Improvement of physico-mechanical and microstructural properties of magnesium phosphate cement composites comprising with Phosphogypsum, J Clean Prod, 261 (2020).
28. N. Muisa, I. Nhapi, W. Ruziwa, M.M. Manyuchi, Utilization of alum sludge as adsorbent for phosphorus removal in municipal wastewater: A review, J Water Process Eng, 35 (2020).
29. N.F. Mihelj, N. Ukrainczyk, S. Leakovic, J. Sipusic, Waste Phosphogypsum - Toward Sustainable Reuse in Calcium Sulfoaluminate Cement Based Building Materials, Chem Biochem Eng Q, 27 (2013) 219-226.
30. P. Kuzmanovic, N. Todorovic, S. Forkapic, L.F. Petrovic, J. Knezevic, J. Nikolov, B. Miljevic, Radiological characterization of phosphogypsum produced in Serbia, Radiat Phys Chem, 166 (2020).
31. P. Sengupta, S. Saha, S. Banerjee, A. Dey, P. Sarkar, Removal of fluoride ion from drinking water by a new $Fe(OH)_3$ nano CaO impregnated chitosan composite adsorbent, Polym-Plast Tech Mat, (2020).
32. R. Zmemla, A. Sdiri, I. Naifar, M. ben Jdidia, B. Elleuch, Tunisian phosphogypsum tailings: Assessment of leaching behavior for an integrated management approach, Environ Eng Res, 25 (2020) 345-355.
33. S. Turkel, E. Aksin, A comparative study on the use of fly ash and phosphogypsum in the brick production, Sadhana-Acad P Eng S, 37 (2012) 595-607.
34. S. Shaddel, T. Grini, S. Ucar, K. Azrague, J.P. Andreassen, S.W. Osterhus, Struvite crystallization by using raw seawater: Improving economics and environmental footprint while maintaining phosphorus recovery and product quality, Water Res, 173 (2020).
35. T. Sun, T. Hu, G.M. Wang, Z.H. Shui, K.Y. Ge, Q.T. Dai, Y.F. Xie, Influence of Clinker and SCMs on Soluble Chemicals and Expansion of Phosphogypsum-Based Cementitious Materials, J Test Eval, 48 (2020) 1950-1961.
36. W. Zhang, F.Z. Zhang, L.P. Ma, P. Ning, J. Yang, Y. Wei, An efficient methodology to use hydrolysate of phosphogypsum decomposition products for CO_2 mineral sequestration and calcium carbonate production, J Clean Prod, 259 (2020).
37. W.M. Kanno, H.L. Rossetto, M.F. de Souza, M.F. Maduar, M.P. de Campos, B.P. Mazzilli, High strength phosphogypsum and its use as a building material, Natural Radiation Environment, 1034 (2008) 307-316.
38. W.J. Ding, Q.J. Chen, H.J. Sun, T.J. Peng, Modified phosphogypsum sequestrating CO_2 and characteristics of the carbonation product, Energy, 182 (2019) 224-235.
39. W.J. Ding, Q.J. Chen, H.J. Sun, T.J. Peng, Modified mineral carbonation of phosphogypsum for CO_2 sequestration, J Co2 Util, 34 (2019) 507-515.
40. W.D. Lu, B.G. Ma, Y. Su, X.Y. He, Z.H. Jin, H.H. Qi, Preparation of alpha-hemihydrate gypsum from phosphogypsum in recycling $CaCl_2$ solution, Constr Build Mater, 214 (2019) 399-412.
41. X. Borgohain, A. Boruah, G.K. Sarma, M.H. Rashid, Rapid and extremely high adsorption performance of porous MgO nanostructures for fluoride removal from water, J Mol Liq, 305 (2020).
42. X.B. Li, Q. Zhang, Z.H. Shen, L.J. Li, X.H. Li, S. Mao, L-aspartic acid: A crystal modifier for preparation of hemihydrate from phosphogypsum in $CaCl_2$ solution, J Cryst Growth, 511 (2019) 48-55.
43. X.L. Xue, Y.X. Ke, Q. Kang, Q.L. Zhang, C.C. Xiao, F.J. He, Q. Yu, Cost-Effective Treatment of Hemihydrate Phosphogypsum and Phosphorous Slag as Cemented Paste Backfill Material for Underground Mine, Adv Mater Sci Eng, 2019 (2019).
44. Y.B. Huang, J.S. Qian, L.C. Lu, W.S. Zhang, S.D. Wang, W.L. Wang, X. Cheng, Phosphogypsum as a component of calcium sulfoaluminate cement: Hazardous elements immobilization, radioactivity and performances, J Clean Prod, 248 (2020).
45. Y.P. Wang, L. Yu, H.P. Yuan, D.W. Ying, N.W. Zhu, Improved removal of phosphorus from incinerated sewage sludge ash by thermo-chemical reduction method with $CaCl_2$ application, J Clean Prod, 258 (2020).
46. Y. Ennaciri, I. Zdah, H. El Alaoui-Belghiti, M. Bettach, Characterization and purification of waste phosphogypsum to make it suitable for use in the plaster and the cement industry, Chem Eng Commun, 207 (2020) 382-392.
47. Y.J. Zhong, T. Shi, Q.G. Chen, X.S. Yang, D.H. Xu, Z.Y. Zhang, X.L. Wang, B.H. Zhong, Leaching calcium from phosphogypsum desulfurization slag by using ammonium chloride solution: Thermodynamics and kinetics study, Chinese J Chem Eng, 28 (2020) 208-215.
48. Z.H. Jin, B.G. Ma, Y. Su, W.D. Lu, H.H. Qi, P.H. Hu, Effect of calcium sulphoaluminate cement on mechanical strength and waterproof properties of beta-hemihydrate phosphogypsum, Constr Build Mater, 242 (2020).

Figures

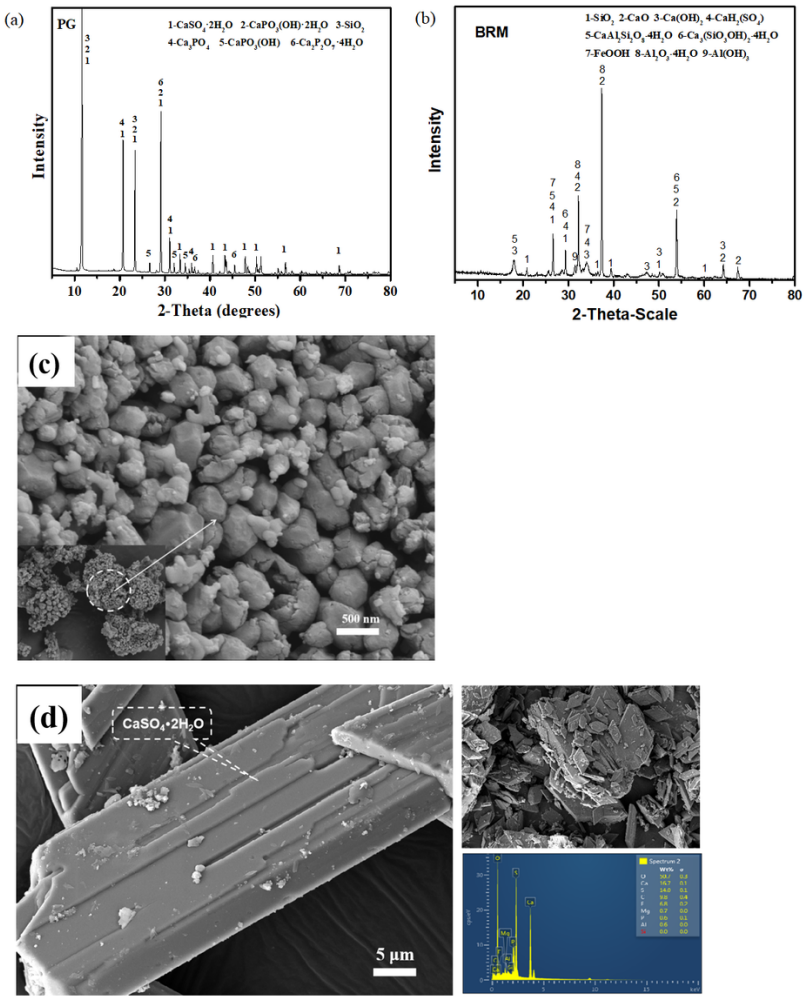

Figure 1

(a) X-ray diffraction of PG; (b)X-ray diffraction of BRM; (c) SEM analysis of BRM; (d) SEM and matching EDS analysis of PG.

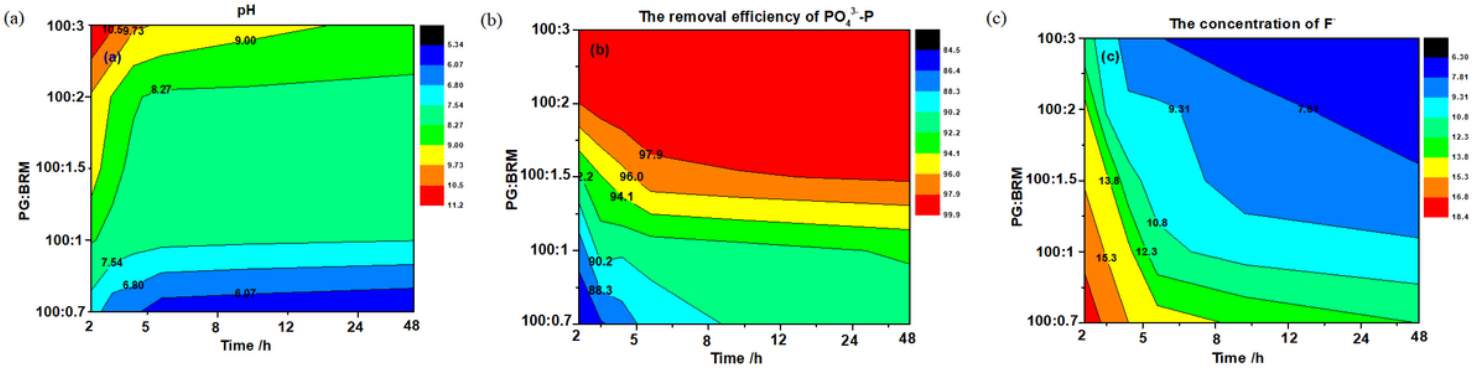

Figure 2

The effects of PG and BRM weight ratios on the concentrations of F-, PO43–P and the pH of leaching solution when the solid to liquid ratio was 4:1 and reaction for 24 h at 30°C: (a) pH;(b) PO43–P; (c) F-.

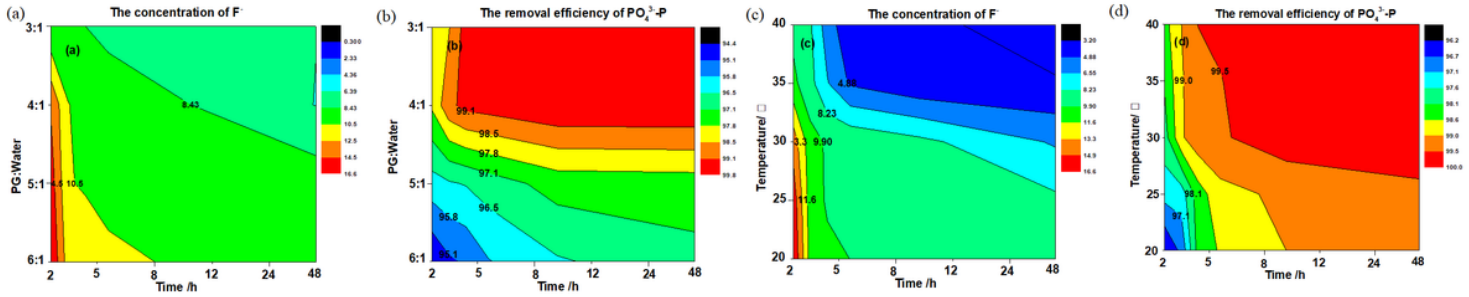

Figure 3

The effects of reaction temperature on the concentrations of F- and PO43–P at the different reaction time and the solid to liquid ratio was 4:1: (a) F-; (b) PO43–P; the effects of solid to liquid ratio on the concentrations of F- and PO43–P at the different raction time when the temperature at 30 ℃: (c) F-; (d) PO43–P.

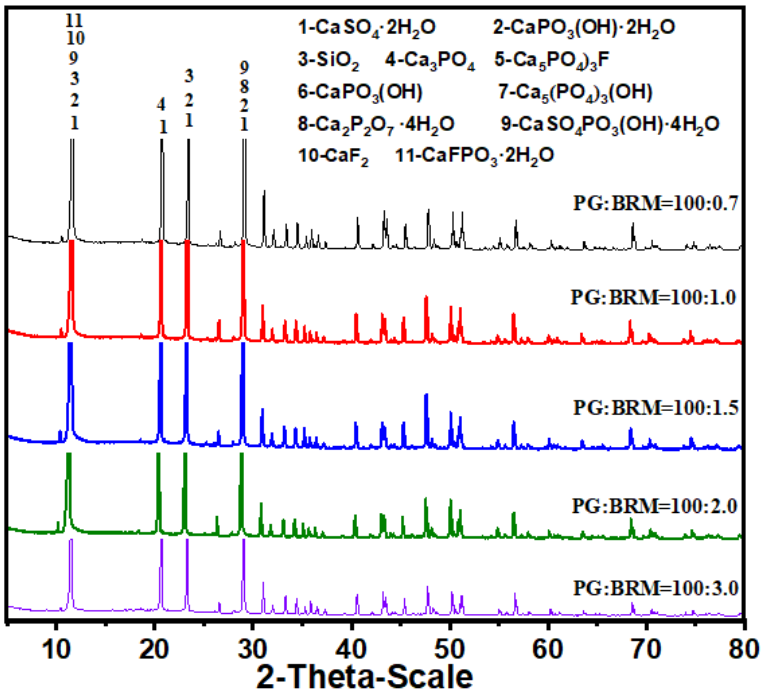

Figure 4

XRD patterns analysis at the different weight ratio of PG and BRM when the solid to liquid ratio was 4:1 and the temperature at 30 ℃ reacting for 24 h.

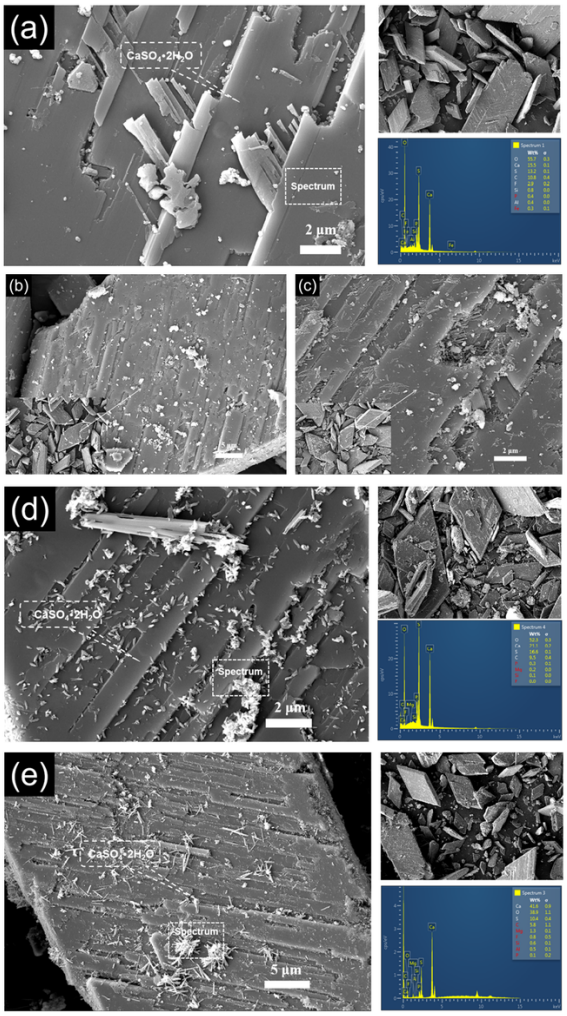

Figure 5

SEM and matching EDX data analysis of precipitate at the different weight ratio of PG and BRM, when the solid to liquid ratio was 4:1 reacting for 24 h and the temperature at 30 °C. (a) 100:0.7; (b)100:1.0; (c)100:1.5; (d)100:2.0; (e)100:3.0.

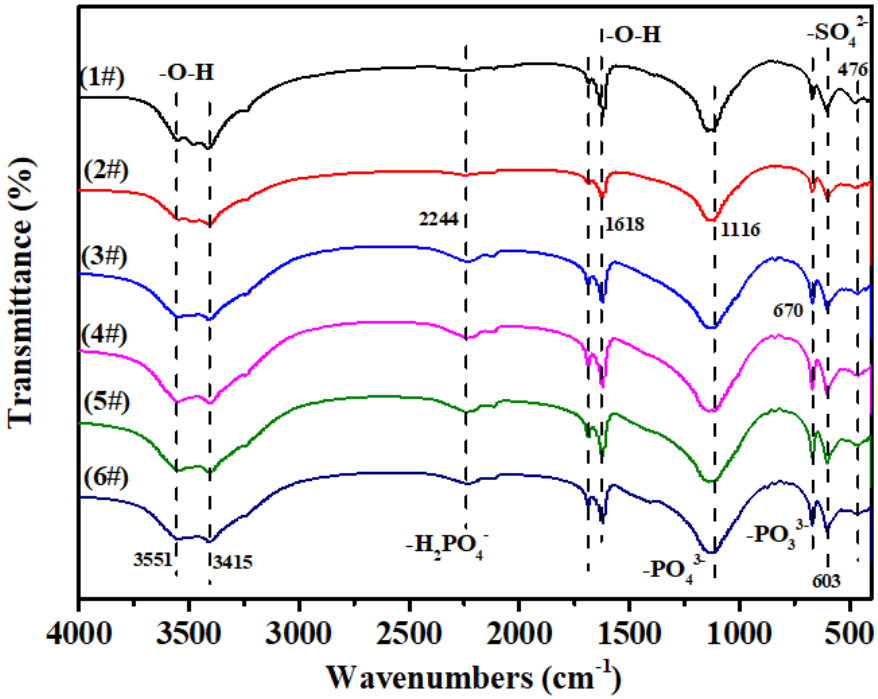

Figure 6

FT-IR spectra of different samples at the different weight ratio of PG and BRM when the solid to liquid ratio was 4:1 reacting for 24 h and the temperature at 30 °C (1#) Raw PG; (2#)100:0.7; (3#)100:1.0; (4#)100:1.5; (5#)100:2.0; (6#)100:3.0.